



A Novel of Nonlinear Voltage Regulators analysis by using Synchronizing and Damping torques

Dr.V.S.Vakula

*Asst. Professor, Head of the Dept. of EEE,
JNTUK UCEV, Vizianagaram, India.*

V.Madhavi

*PG Student, Dept. of EEE,
JNTUK UCEV, Vizianagaram, India.*

Abstract- *This paper presents an approach to replace the conventional excitation system (AVR+PSS) with a nonlinear voltage regulators derived using synchronizing and damping torque analysis. Now-a- days a keen interest has been developed in designing nonlinear exciters to provide a good dynamic performance in the complex environment of a power system. A feedback linearization technique is used to design two nonlinear controllers that uses nonlinear control laws for derivation and analysis. The performance of two regulators are tested for different operating cases on linearized model of Heffron Phillip's model has developed and the synchronizing and damping torques are analyzed to study the nature of small signal stability*

Keywords: *Feedback linearization, small signal stability, single machine infinite bus system, synchronizing and damping torques*

1. INTRODUCTION

The excitation control system plays prominent role in power systems. Many controllers have been developed to control the terminal voltage, but there is a considerable development in nonlinear controller designs which uses various controlling techniques such as feedback linearization, back stepping, and variable structure control, synergy control theory, etc. [1]-[11]. These control designs aims to replace the conventional excitation system (AVR+PSS) . the first design of the nonlinear control design is proposed in [12]. Out of all these control designs Feedback linearization technique is widely used for generator excitation system [6] [7] [12-17]. All the nonlinear control designs presents the excitation control problem as regulator problem. Two nonlinear voltage regulators are considered from [6] and [7], which are two different approaches of Feedback linearization utilizes terminal voltage V_t as the design objective. Even though these nonlinear voltage regulators improves transient stability but shows a poor performance regarding the small signal stability [18]. This paper postulates the merits and demerits of the two nonlinear voltage regulators that can be able to replace the conventional excitation system. In [6] the nonlinear control law is derived by using the derivative of the terminal voltage which uses input – output feedback linearization technique. The state variables are rotor angle δ , slip speed S_m and transient induced voltage due to field flux-linkages E_q' and in [7] the nonlinear control law is derived by cancellation of nonlinearities present in the derivative of the active power equation of SMIB and uses input state feedback linearization method. The state variables for these controller are terminal voltage V_t and slip speed S_m and generator active power P_g . To access the small signal behavior all the nonlinear control laws derived are linearized around an operating condition and the developed model is called Heffron Phillip's model which is quite similar to the high gain static automatic voltage regulator but it has positive feedback signal from the speed deviations acts like stabilizing signal just like power system stabilizers which damp out the oscillatory instability signal. From these model synchronizing and damping torques are developed for these nonlinear voltage regulators. Under weak system conditions the damping torque of the nonlinear voltage regulator in [6] reduces with increase in system loading and its reactance and becomes negative finally. These nonlinear AVR is better than static AVR but not over the conventional excitation system (AVR+PSS) where as the nonlinear voltage regulator in [7], the damping term coefficient increases with system loading and its equivalent reactance which is quite opposite to the nonlinear AVR in [6] makes to replace the entire AVR+PSS over a wide range of operating conditions.

II. MODELLING OF A POWER SYSTEM

IEEE model 1.0 is considered to represent the synchronous generator in [6] and [7] of a SMIB. The third order nonlinear dynamics equations governing the SMIB are follows

$$\frac{d\delta}{dt} = w_B S_m \quad (1)$$

$$\frac{dS_m}{dt} = \frac{1}{2H} \{T_{mech} - T_{elec} - DS_m\} \quad (2)$$

$$\frac{dE'_q}{dt} = \frac{1}{T'_{do}} \{-E'_q + (X_d - X'_d)i_d + E_{fd}\} \quad (3)$$

$$T_{elec} = E'_q i_q + (X'_d - X_d)i_d i_q \quad (4)$$

The objective is to design a nonlinear control law for field winding voltage E_{fd} which makes the terminal voltage tends to the pre specified voltage V_{ref}

NONLINEAR VOLTAGE REGULATOR [6]

In [6] the nonlinear control law is derived till the control input E_{fd} appears in the derivative of the terminal voltage. Here the number of iterations in the derivative is one it means that the relative degree is one .The terminal voltage of the SMIB as follows by letting $R_a = 0$

$$V_t = \sqrt{\left[\left(\frac{X_q E_b \sin \delta}{X_e + X_q}\right)^2 + \left(\frac{X'_d E_b \cos \delta + X_e E'_q}{X_e + X'_d}\right)^2\right]} \quad (5)$$

By applying derivative we get

$$\dot{V}_t = \left\{ \frac{1}{\sqrt{V_t}} (V_d C_{11} w_B S_m \cos \delta - \delta \dot{V}_d C_{22} E_b \sin \delta) + \frac{1}{\sqrt{V_t}} \frac{V_q C_{33}}{T'_d} (-E'_q + (X_d - X'_d)i_d) \right\} + \left\{ \frac{1}{\sqrt{V_t}} \frac{V_q C_{33}}{T'_d} \right\} E_{fd} \quad (6)$$

where $C_{11} = \frac{X_q}{X_e + X'_q}$ $C_{22} = \frac{X'_d}{X_e + X'_d}$ $C_{33} = \frac{X_e}{X_e + X'_d}$ (7)

Equation (6) can also be written as $\dot{V}_t = f(x) + g(x)u$ (8)

With the solvation of error dynamics the nonlinear control law for E_{fd} as follows

$$E_{fd} = \frac{T'_{do}}{C_3 V_q} \left[-K_v (V_t - V_{ref}) \sqrt{V_t} - (V_d C_{11} \cos \delta w_B S_m E_b) + V_q C_{22} E_b \sin \delta w_B S_m \right] + E'_q - (X_d - X'_d)i_d \quad (9)$$

K_v is the only tuned parameters that can make the machine behave nonlinearly when applied to the closed control loop. The designed nonlinear AVR is tested for few test cases and machine data is taken from [18] where steam is the input.

CASE – I

The step change of 0.1 p.u in V_{ref} in terms of rotor angle δ are tested on static AVR, static AVR+PSS and FBLAVR with $K_v = 20$ for a system data of $P_g + jQ_g = 1+j0.2$, $X_e = 0.4$ and by keeping terminal voltage and infinite bus voltage 1 p.u The results are shown in fig 1.

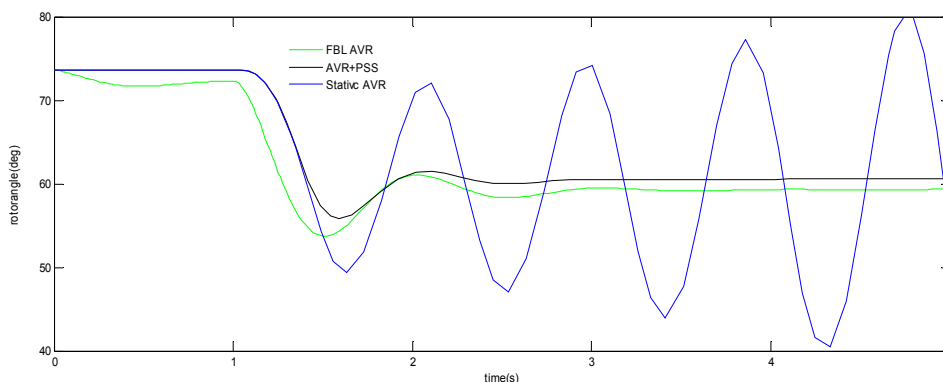


Fig 1 Step response of δ for 10% change in V_{ref}

CASE – II

The following changes are noticed in fig 2 when there is a 0.1 p.u step change in T_m are tested on static AVR+PSS and FBLAVR for a system data of $P_g + jQ_g = 1+j0.8$ and $X_e = 0.8$, $V_t = 1$ p.u.

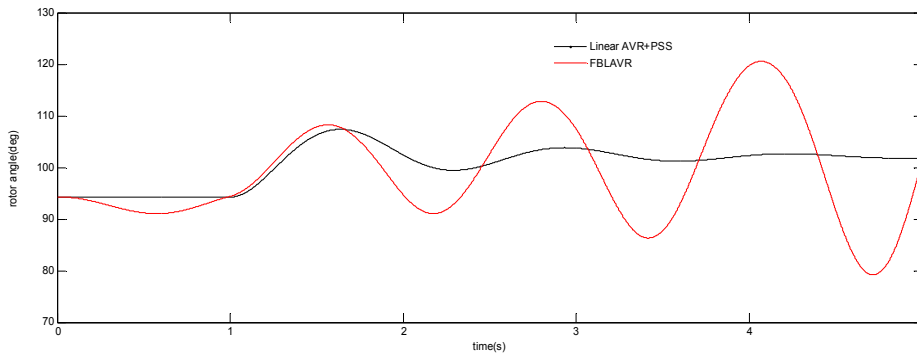


Fig 2. Step response of δ for 10% step change in T_m

SMALL SIGNAL ANALYSIS

To study the small signal analysis of the nonlinear controller [6], the nonlinear control law is linearized by using Taylor series approximation. By linearizing (9) gives

$$\Delta E_{fd} = \frac{T'_{do}}{C_{33}V_{q0}} \left[-K_v(\Delta V_t - \Delta V_{ref})\sqrt{V_{ref}} + (V_{q0}C_{22}E_b \sin \delta_0 \omega_B - V_{do}C_{11}E_b \cos \delta_0 \omega_B)\Delta S_m \right] + \Delta E'_q - (X_d - X'_d)\Delta i_d \tag{10}$$

Δi_d and $\Delta E'_q$ are linearized to give

$$\Delta V_t = K_5 \Delta \delta + K_6 \Delta E'_q \tag{11}$$

$$\Delta i_d = C_1 \Delta \delta + C_2 \Delta E'_q \tag{12}$$

where

$$K_5 = -\frac{X_q V_{do} E_b \cos \delta_0}{(X_q + X_e)V_{ref}} - \frac{X'_d V_{q0} E_b \sin \delta_0}{(X_e + X'_d)V_{t0}} \tag{13}$$

$$K_6 = \frac{X_{te}}{X_e + X'_d} \frac{V_{q0}}{V_{t0}} \tag{14}$$

$$C_1 = \frac{1}{A} [R_t V_{s0} \cos \delta_{s0} - (X'_q + X_t)V_{s0} \sin \delta_{s0}] \tag{15}$$

$$C_2 = -\frac{1}{A} (X'_q + X_t) \tag{16}$$

$$A = (X_e + X'_d)(X_q + X_e) + R_e^2 \tag{17}$$

By substituting the (11) and (12) in (10) we get

$$\Delta E_{fd} = \frac{T'_{do} K_v \sqrt{V_{t0}}}{C_{33} V_{q0}} \times \left\{ \begin{aligned} & \left[-\left[\frac{K_5 + \frac{(X_d - X'_d)V_{q0}C_{33}C_1}{T'_d K_v \sqrt{V_{t0}}}}{G_5} \Delta \delta - \left[\frac{C_{33}V_{q0}}{T'_d K_v \sqrt{V_{t0}}} + \frac{(X_d - X'_d)V_{q0}C_{33}C_2}{T'_d K_v \sqrt{V_{t0}}} + K_6 \right] \Delta E'_q \right] \right. \\ & \left. + \Delta V_{ref} + \frac{(\Gamma_2 - \Gamma_1)}{K_v \sqrt{V_{t0}}} \Delta S_m \right] \end{aligned} \right\} \tag{18}$$

where $\Gamma_1 = V_{q0} \omega_B C_{22} E_b \sin \delta_0$ and $\Gamma_2 = V_{do} \omega_B C_{11} E_b \cos \delta_0$

the equation (18) can also written as

$$\Delta E_{fd} = K_{FBL} [-G_5 \Delta \delta - G_6 \Delta E'_q + \Delta V_{ref} + G_D \Delta S_m] \tag{19}$$

The above equation (19) is represented in the block diagram shown in fig 3.

The above block shown in fig 3 is similar to that of high gain static AVR, but there is additional component called G_D for speed deviations and it is a fast acting nonlinear AVR with a gain of KFBL and low time constant. The negatively affected torque angle loop consists of two components one to deviations of the rotor angle $\Delta \delta$ and it is denoted by G_5 and another due to deviations in due to flux linkages E'_q denoted by G_6 and additional component G_D due to deviations in slip speed S_m . The terms G_5 and G_6 are analogues to the terms K_5 and K_6 of a Heffron Phillip's constant model of a SMIB system. The behavior of the G_5 and G_6 along with K_5 and K_6 are studied by varying P_g from 0.5 to 1 and X_e from 0.2 to 0.8 by keeping terminal voltage and infinite bus voltage 1 p.u and fixing the gain parameter $K_v = 20$. In the same process G_D is also studied.

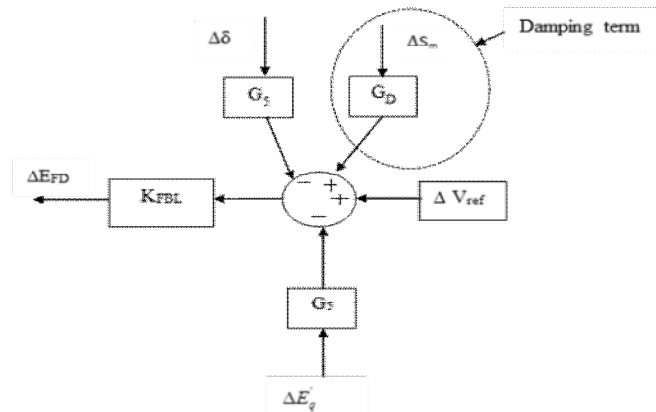


Fig 3 Output feedback linearization based AVR

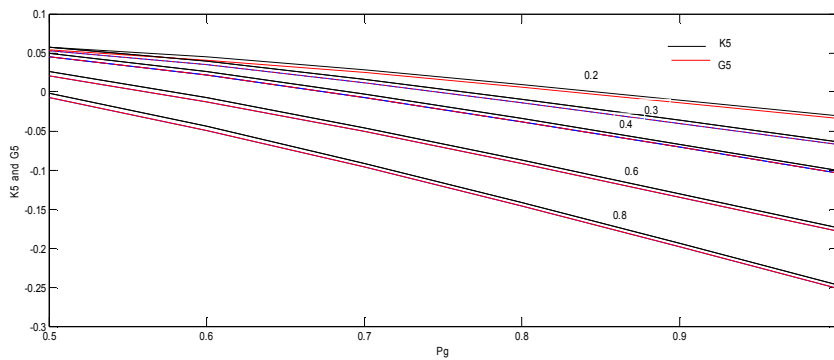


Fig 4 Variation of G_5 and K_5 with P_g for various values of X_e

It can be said from the fig 4 the nature of G_5 and K_5 are similar .It may be positive or negative depending upon the system loading conditions.

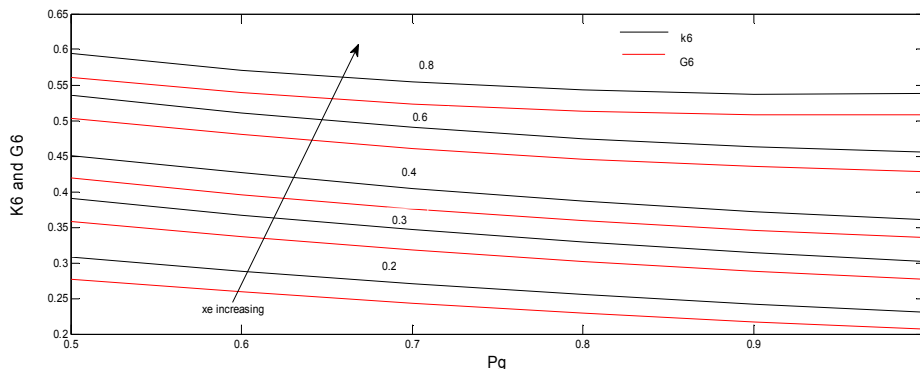


Fig 5 Variation of G_6 and K_6 with P_g for various values of X_e

Fig 5 says that for all operating conditions G_6 and K_6 are positive

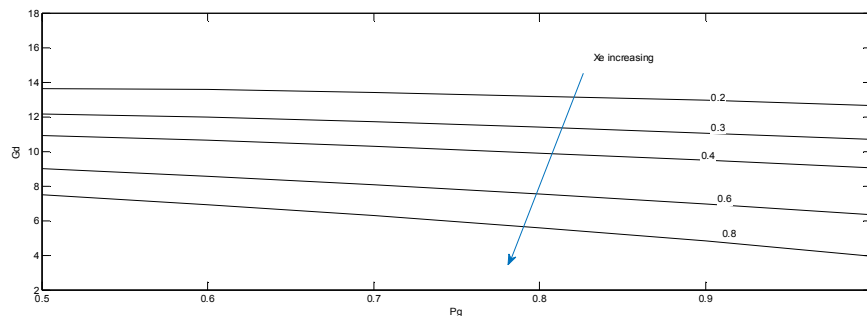


fig 6 Variation of G_D with P_g for various values of X_e

In fig 6, variation of G_D with P_g for various values of X_e says that there is a decrement in G_D with increase in system loading and its reactance which makes the nonlinear AVR to fail when operated in weak systems and heavy loading conditions

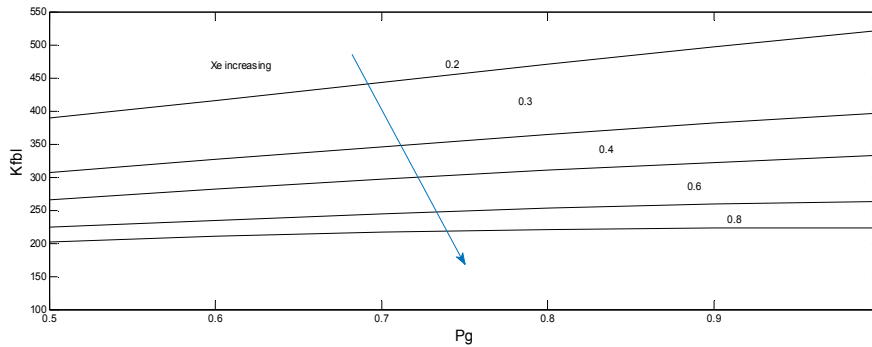


Fig 7 Variation of K_{FBL} with P_g for various values of X_e

From fig 7 we can say that the range of K_{FBL} lies between 200 to 500 which is the typical range of linear AVR by varying P_g and X_e

SYNCHRONIZING AND DAMPING TORQUE ANALYSIS

The analysis of synchronizing and damping torque is done by using the Heffron Phillip’s model developed for nonlinear AVR and shown in fig 8. The electrical torque T_e through E_q' can be represented as [22]

$$\Delta T_{e2} = \frac{K_2 K_3 [-K_4 - K_{FBL} G_5] \Delta \delta}{1 + s T_{elec1}} + \frac{K_2 K_3 G_D \Delta S_m}{1 + s T_{elec2}} \quad (20)$$

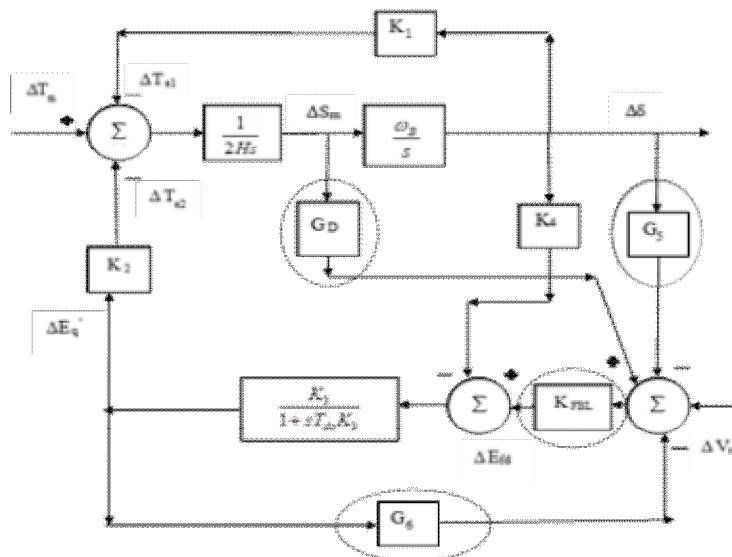


Fig 8 Heffron Phillip’s model including FBLAVR

The component $Telec1$ is a linear part because the torque is produced by the linear AVR is with a gain of K_{FBL} and low time constant. The component $Telec2$ is a nonlinear part, here the torque is produced by the G_D due to nonlinear AVR action. The equations governing the Heffron Phillip’s model can also be represented in the form of state space equations and system matrix A_{FBL} is

$$A_{FBL} = \begin{bmatrix} 0 & W & 0 \\ \frac{-K_1}{2H} & \frac{-D}{2H} & \frac{-K_2}{2H} \\ \frac{-(K_4 + K_{FBL} G_5)}{T'_{do}} & \frac{(K_{FBL} G_D)}{T'_{do}} & \frac{1 + K_{FBL} G_6}{T'_{do}} \end{bmatrix} \quad (21)$$

From these system matrix AFBL Eigen values are computed and by substituting $s = a + jb$ and $\Delta S_m = \frac{s\Delta\delta}{\omega_o}$ in (20) we get

$$T_S = \underbrace{Re \{T_{elec1}\}}_{Linear\ part} + \underbrace{\left(\frac{-a}{b}\right) Im \{T_{elec1}\}}_{Linear\ part} + \underbrace{Im \{T_{elec2}\}}_{Nonlinear\ part} \left(\frac{-a^2}{b} - \frac{b}{a}\right) \quad (22)$$

$$T_D = \underbrace{Im \{T_{elec1}\}}_{Linear\ Part} \frac{W_0}{b} + \underbrace{Re \{T_{elec2}\}}_{Nonlinear\ part} + \underbrace{Im \{T_{elec2}\}}_{Nonlinear\ part} \frac{a}{b} \quad (23)$$

For various different operating conditions the parameters K_4 and K_2 are positive and G_5 may be positive or negative depending upon the loading conditions and the total synchronizing torque is obtained by adding K_1 to the T_s in (22). Letting $G_D = 0$ the equations (18) and (19) represents the linear AVR with gain $K_A = K_{FBL}$. Fig 9 and 10 shows the linear parts of T_s and T_D variation by varying P_g from 0.5 to 1 along with X_e from 0.2 to 0.8

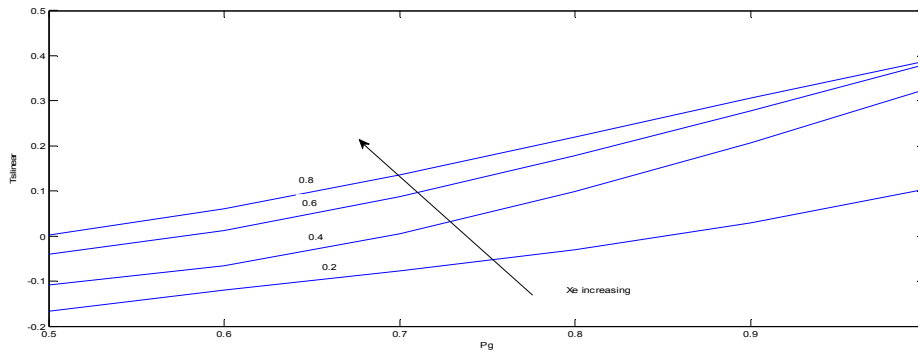


Fig 9 T_s contribution due to linear part of the controller

It can be realized from the fig 9 that the linear AVR fails to produce synchronizing torque under heavy and light load conditions.

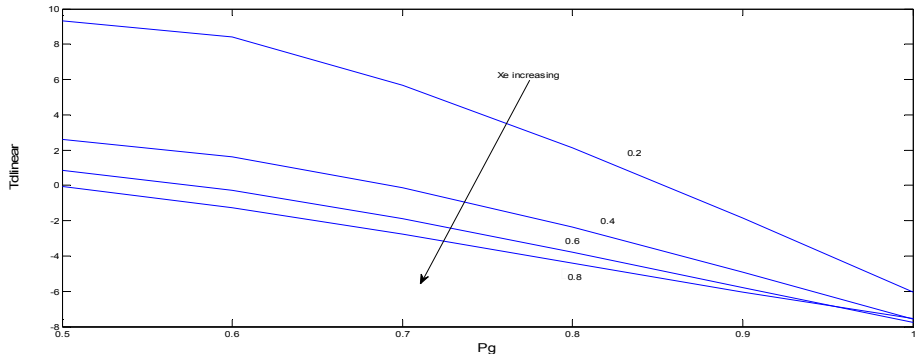


Fig 10 T_D contribution due to linear part of the controller

It can be referred from fig 10, the damping torque due to linear part of T_D decreases with increase in X_e and finally becomes negative when G_5 becomes negative.

It makes the linear AVR to fail under weak loading and heavy loading conditions due to presence of negative damping torque. The variation of synchronizing and damping torque components contributed from the nonlinear part solely depends upon the G_D component alone.

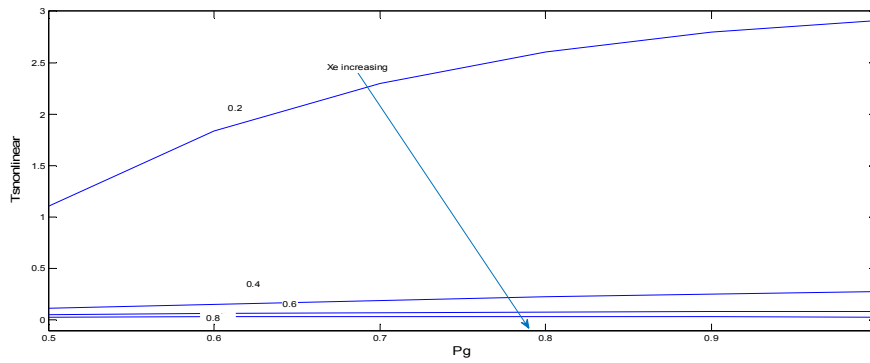


Fig 11 T_s contribution due to nonlinear part of the controller

Fig.11. describes the positive nature during overall operating range. Higher values of T_s under strong system is a desirable feature. The positive T_s values over the whole range indicates that the G_D component always aids the total T_s .

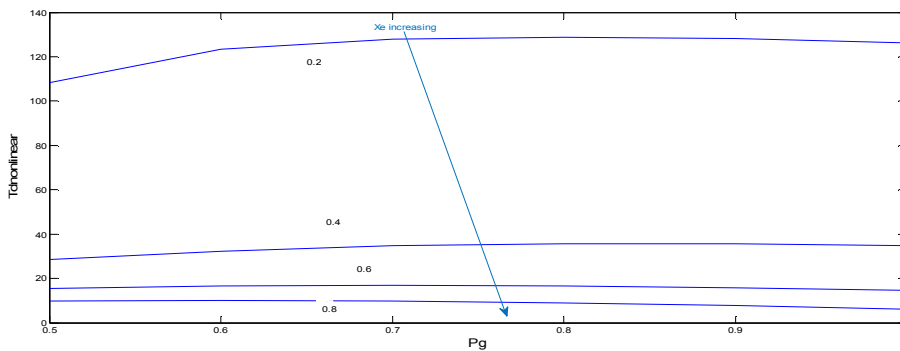


Fig 12 T_D contribution due to nonlinear part controller [6]

Fig.12.the value damping torque is less during weak conditions and it may not sufficient to counteract the damping contribution from the linear part.

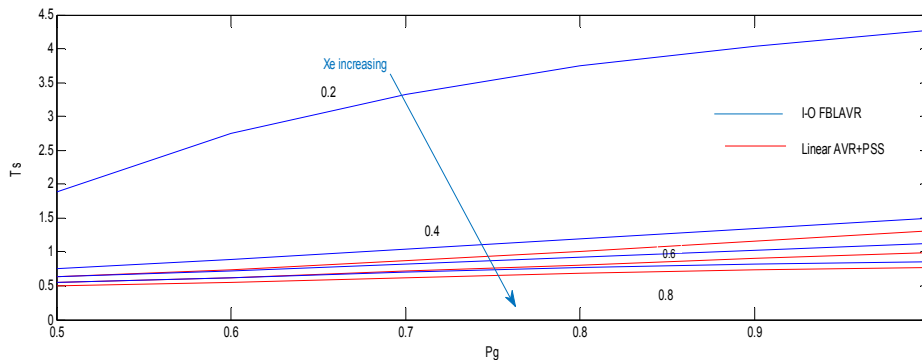


Fig 13 Total T_s contribution of controller proposed in [6] and linear AVR+PSS

The behavior of the I-O FBLAVR is similar to the linear AVR+PSS. Total contribution of T_s is much higher than the linear AVR+PSS

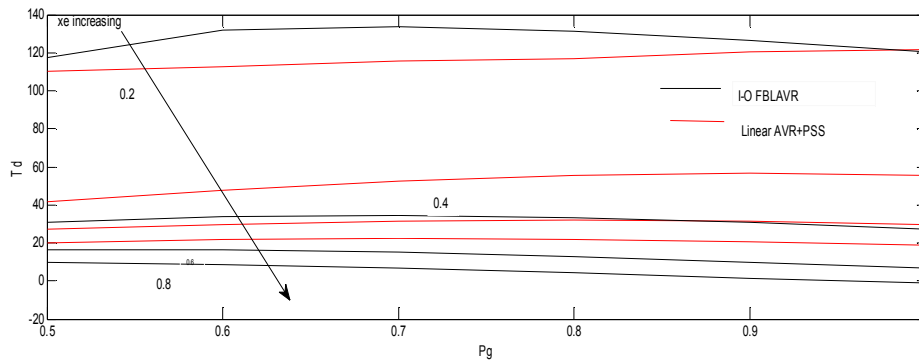
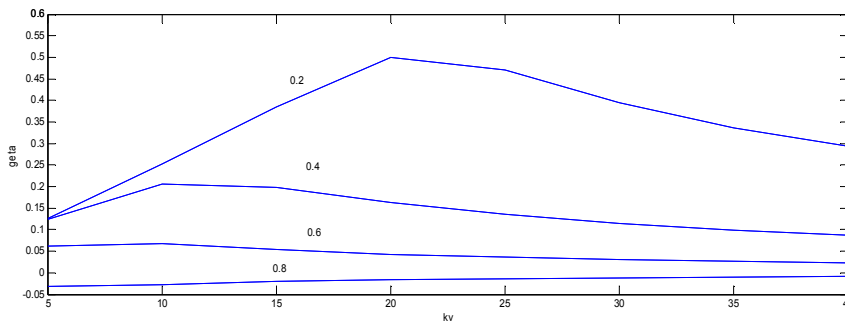


Fig 14. Total T_D contribution of the controller proposed in [6] and linear AVR+PSS

Fig. 14. shows the contribution of total T_D is not as good when compared with linear AVR+PSS expect for $X_e = 0.2$ p.u. and also the total T_D becomes negative for $X_e = 0.8$. There by it reveals the poor performance under heavy and light loaded conditions. The damping term ζ is calculated by using total synchronizing and damping torques and it as follows

$$\zeta = \frac{1}{2} \frac{T_D}{\sqrt{T_s} 2H\omega_B} \quad (24)$$

Fig. 15 shows the variation ζ of with increase in K_v for various values of external reactance by keeping the real power and terminal voltage constant i.e, $P_g + jQ_g = 1 + j0.2$. It can be observed that for each X_e value, the damping factor increases with increase in K_v , reaches maximum for some K_v and then starts decreasing. The value K_v of at which maximum damping occurs decreases with increase in X_e . From referring all simulation results we can say that the nonlinear AVR can not repalce the entire AVR+PSS system for over all operating conditions because its performance is poor under heavy and light load conditions due its negative damping torque effect.



III. NONLINEAR VOLTAGE REGULATOR [7]

The synchronous generator in SMIB of third order model is considered to design the nonlinear voltage regulator in [7]. In these input state feedback linearization techinque is used. Here the nonlinear control law is derived by cancelling the nonlinearities present in the derivative of active power of a synchronous generator .A new input V_f is derived by considering terminal voltage V_t , Slip speed S_m , and active power P_g has state variables. It is a full state feedback controller.

The active power of a synchronous generator is given by

$$P_g = \frac{E'_q E_b \sin \delta}{X_q + X_e} \quad (25)$$

By applying derivative to P_g we get

$$\dot{P}_g = \frac{E'_q E_b \sin \delta}{X_q + X_e} + \frac{E'_q E_b \cos \delta}{X_q + X_e} \dot{\delta} \quad (26)$$

By rearranging the terms (26) transforms to

$$\dot{P}_g = -\frac{P_g}{T'_{do}} + \frac{1}{T'_{do}} \left\{ I_q [E_{fd} + (X_d - X_q)I_d + T'_{do} \frac{E'_q E_b \cos \delta}{X_q + X_e} \omega_B S_m] \right\} \quad (27)$$

Their by the new input V_f is

$$V_f = I_q [E_{fd} + (X_d - X_q)I_d] + T'_{do} \frac{E'_q E_b \cos \delta}{X_q + X_e} w_B S_m - P_m \quad (28)$$

By using these new input V_f the nonlinearities present in (27) are cancelled and it takes form of

$$\dot{x} = -\frac{P_g - P_m}{T'_{do}} + \frac{1}{T'_{do}} V_f \quad (29)$$

With the help of these equations one can derive the nonlinear control law E_{fd} as follows

$$E_{fd} = \frac{1}{I_q} \left[V_f - T'_{do} \frac{E'_q E_b \cos \delta}{X_q + X_e} w_B S_m + P_m \right] - (X_d - X_q) I_d \quad (30)$$

These state space equation that is formulated by using the new control variable V_f is

$$\dot{x} = Ax + BV_f \quad (31)$$

$$\text{where } A = \begin{bmatrix} 0 & f_1 & -f_2 \\ 0 & \frac{-D}{2H} & -\frac{w_B}{2H} \\ 0 & 0 & -\frac{1}{T'_{do}} \end{bmatrix} \quad (32)$$

$$B = \begin{bmatrix} \frac{f_2}{T'_{do}} & 0 & \frac{1}{T'_{do}} \end{bmatrix} \quad (33)$$

$$f_1 = \frac{P_g^2 X_e^2 \cos \delta}{V_t E_b^2 \sin^3 \delta} - \frac{X_e X_q P_g}{V_t (X_q + X_e) \sin^2 \delta} \quad (34)$$

$$f_2 = \frac{P_g X_e^2}{V_t E_b^2 \sin^2 \delta} + \frac{X_e X_q \cos \delta}{V_t (X_q + X_e) \sin \delta} \quad (35)$$

The new input V_f can be written as

$$V_f = -K_v \Delta V_t - K_w w_B \Delta S_m - K_p \Delta P_g \quad (36)$$

The final modified form of nonlinear control law E_{fd} is

$$E_{fd} = \frac{1}{I_q} \left[-K_v \Delta V_t - K_w w_B \Delta S_m - K_p \Delta P_g - T'_{do} \frac{E'_q E_b \cos \delta}{X_q + X_e} w_B S_m + P_m \right] - (X_d - X_q) I_d \quad (37)$$

Small signal analysis

To study the behavior of nonlinear AVR for small signal analysis the nonlinear control law is linearized around an operating condition and we get

$$\Delta E_{fd} = \frac{1}{I_{q0}} \left[-K_v \Delta V_t + K_v \Delta V_{ref} - K_w w_B \Delta S_m - K_p \Delta P_g - T'_{do} \frac{E'_{q0} E_b \cos \delta}{X_q + X_e} w_B \Delta S_m - E'_{q0} \Delta I_q \right] - (X_d - X_q) \Delta I_d \quad (38)$$

ΔP_g and ΔI_q are linearized to get [21]

$$\Delta P_g = K_1 \Delta \delta + K_2 \Delta E'_q \quad (39)$$

$$\Delta I_q = C_3 \Delta \delta + C_4 \Delta E'_q \quad (40)$$

$$\text{where } C_3 = \frac{1}{A} [(X'_d + X_e) E_b \cos \delta_0 + R_e E_b \sin \delta_0] \quad (41)$$

$$C_4 = \frac{R_e}{A} \quad (42)$$

By substituting (39) (40) in (38) finally we derive E_{fd} is

$$\Delta E_{fd} = \frac{K_V}{I_{q0}} \left\{ \begin{aligned} & - \left[K_5 + \frac{K_p}{K'} K_1 + \frac{C_3 E'_{q0}}{K'} + \frac{(X_d - X_q) C_1 I_{q0}}{K'} \right] \Delta \delta \\ & + \left[\frac{K_w - T'_{do} E'_{q0} E_b \cos \delta}{K' (X_d + X_q)} \right] w_B \Delta S_m \\ & - \left[K_6 + \frac{K_p}{K'} K_2 + \frac{C_4 E'_{q0}}{K'} + \frac{(X_d - X_q) C_2 I_{q0}}{K'} \right] \Delta E'_q \\ & + \Delta V_{ref} \end{aligned} \right\} \quad (43)$$

The nonlinear control law in (43) is similar to that of (18) and block diagram of fig 3 can be applicable to any nonlinear regulator as its main function is to produce required amount of damping torque. The parameters G_5 , G_6 , G_D are analyzed for various values of X_e by varying P_g from 0.4 to 1 and the system data is taken from [7]

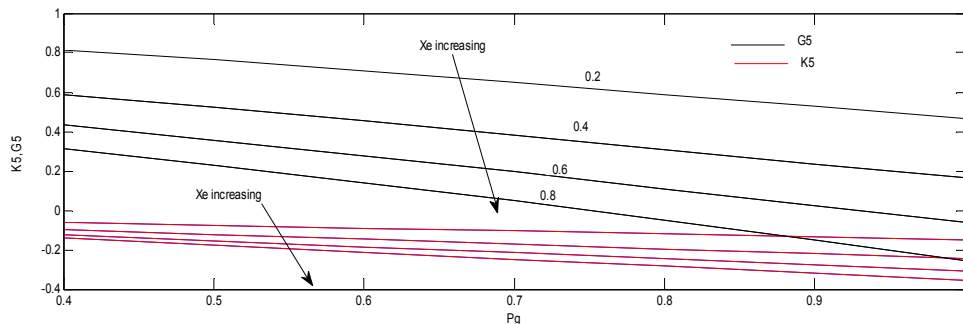


Fig. 16 Variation of G_5 , K_5 , with P_g for the nonlinear AVR proposed in [7]

The variation in G_5 is positive for most of the operating conditions. Even though there is reduction in synchronizing torque due to positive behaviour but it helps from negative damping effect. The variation of G_6 is always positive under all operating conditions and also the difference between the K_6 and G_6 is high, but the increase in G_6 does not show any significant effect on damping torque. The variation of damping term G_D increases with X_e and P_g . This is the most desirable feature where linear AVR + PSS fails under weak system conditions and heavy loading.

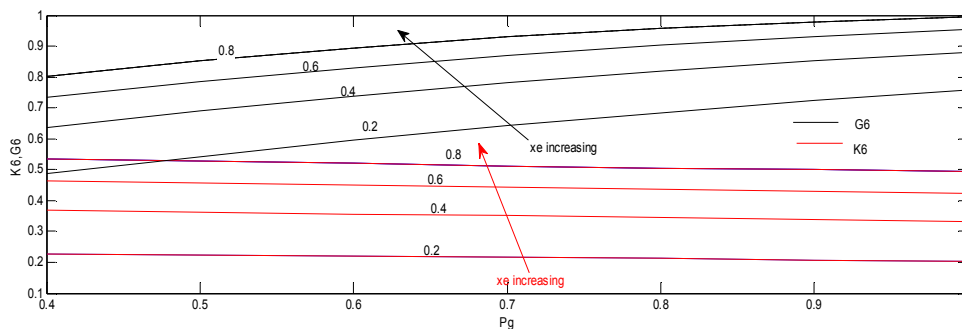


Fig. 17 Variation of G_6 , K_6 , with P_g for the nonlinear AVR proposed in [7]

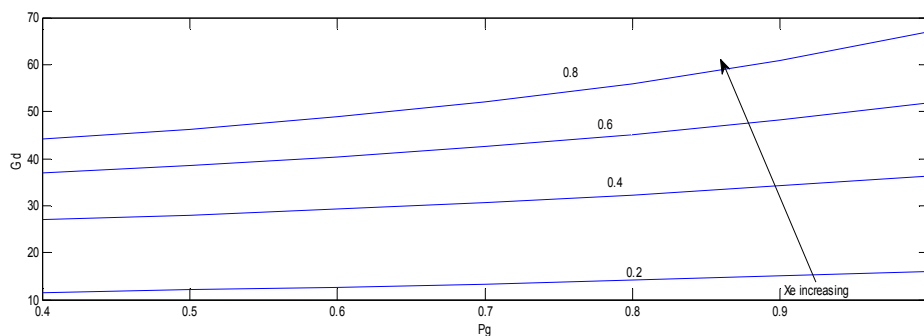


Fig 18 Variation of G_D with P_g for the nonlinear AVR proposed in [7]

SYNCHRONIZING AND DAMPING TORQUES ANALYSIS

The analysis for synchronizing and damping torques are similar as proposed in [6]. The linear parts contributed by the T_S and T_D are consistent according to [18]. T_S and T_D due to nonlinear part are positive with increasing X_e which is opposite behaviour of the controller[6].

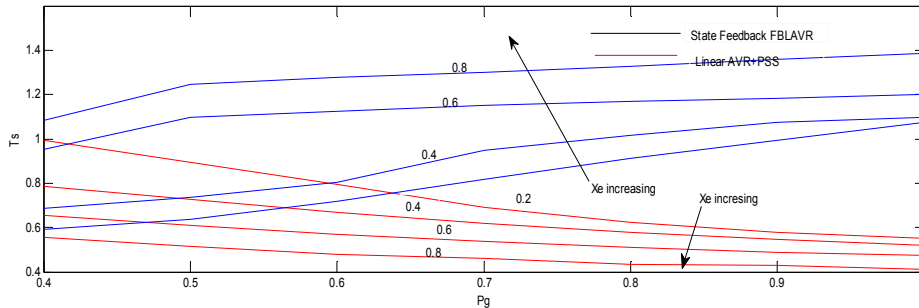


Fig 19 Total T contribution of controller proposed in [7] and linear AVR+PSS

The fig 19, variations in T_S are exactly opposite to linear AVR+PSS.

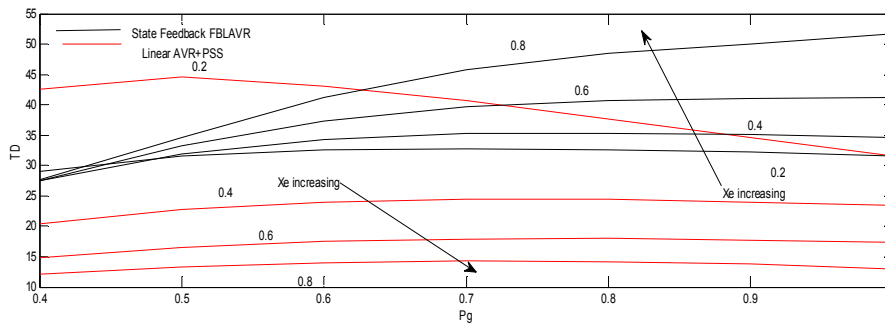


Fig 20 Total T_D contribution of controller proposed in [7] and linear AVR+PSS

Fig.20 shows that damping torque T_D which is opposite to the damping torque of the Linear AVR+PSS. The Fig.20. shows that the damping ratio increases with increase in X_e and remains constant with loading above 0.7 p.u.

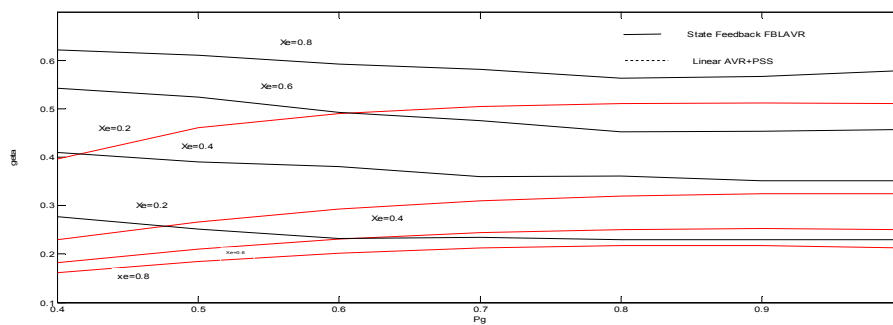


Fig.20 Variation of damping factor ζ with P_g for various values of X_e

SINGLE TUNABLE PARAMETER

The above two proposed nonlinear voltage regulators are good when they are worked on Single machine infinite bus system (SMIB). By adding one parameter to the control law [6] i.e., G_{VS} . It can be used in the area of multi-machine system. The nonlinear control law modifies to

$$\Delta E_{fd} = \frac{T_{d0} k_v \sqrt{V_{t0}}}{C_{33} V_{q0}} \left[\begin{aligned} & - K_5 \Delta \delta - \left[\frac{(x_d - x'_d) v_{q0} c_{33} c_1}{G_5} \right] \Delta \delta \\ & - \left[K_6 - \frac{c_{33} v_{q0}}{T_{d0} k_v \sqrt{V_{t0}}} + \frac{(x_d - x'_d) v_{q0} c_{33} c_2}{G_6} \right] \Delta E_q \\ & + \Delta v_{ref} + \frac{(\Gamma_1 - \Gamma_2)}{G_d} \Delta S_m - \frac{(x_d - x'_d) v_{q0} c_{33} c_3}{G_v} \Delta v_s \end{aligned} \right] \quad (45)$$

Where

$$c_3 = \frac{\cos \delta_0}{x_e + x'_d} \quad (46)$$

$$G_{vs} = \frac{(x_d - x'_d) V_{q0} C_{33} C_3}{T_{d0} K_v \sqrt{V_{t0}}} \quad (47)$$

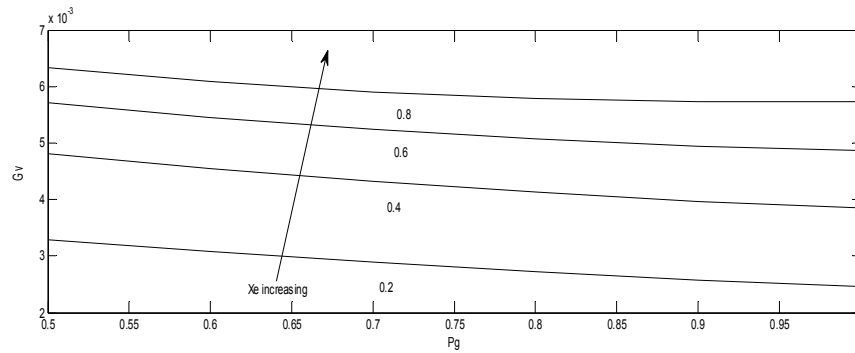


Fig.21. Variation of G_{vs} with X_e

The variation of G_{vs} is plotted by varying P_g and X_e . It generally represents the deviation of voltage magnitudes at high voltage buses. The increase in P_g shows the negative behaviour at different values of X_e .

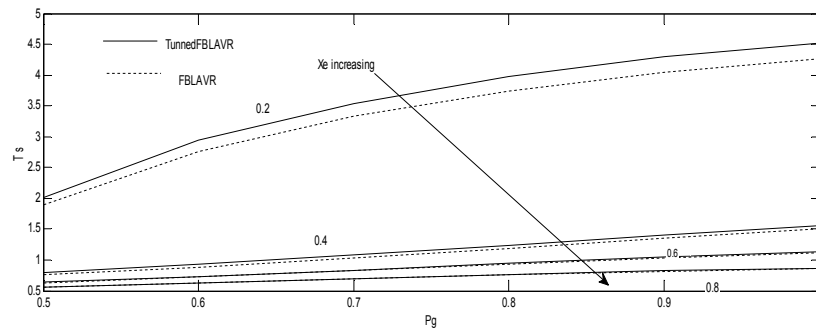


Fig. 22 Total T_s by varying P_g and X_e

It can be observed that total T_s variation is similar to T_s of the nonlinear AVR [6] expect at $X_e = 0.2$.

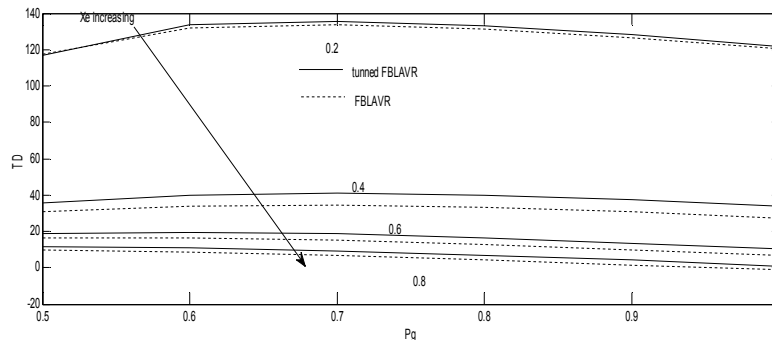


Fig. 23 Total TD by varying P_g and X_e

The total TD variation increases with increase in P_g and X_e . The positiveness of the TD make to operate on entire range of operating conditions.

IV. CONCLUSION

This work attempts to quantify the merits and demerits of the two nonlinear voltage regulators that can successfully replace the existing conventional system. Out of the several transformation techniques to convert nonlinear control laws to linear Feedback linearization is used. The two nonlinear voltage regulators are tested on SMIB system. The performance of the nonlinear AVR proposed in [6] gives better results when compared to Linear AVR+PSS under strong and nominal conditions, but it fails under heavy loading and weak system conditions. The negative damping effect produced by the AVR is the main cause that makes the nonlinear AVR failed to operate under high loads and weak system conditions. Small signal stability is especially poor under weak system conditions. So all the above reasons made the nonlinear AVR not applicable for the entire range of operations and can't be made to replace linear AVR+PSS for entire range of operation. The nonlinear AVR proposed in [7] shows better results and it can entirely replace the conventional excitation system. So the computation of synchronizing and damping torques can assess nature of small signal performance which are tested on single machine bus systems. The dynamic behavior can be enhanced by introducing a suitable tuning parameter that made the nonlinear AVR to work under multi machine systems

V. REFERENCES

- [1]. J. W. Chapman, M. D. Ilic, C. A. King, L. Eng, and H. Kaufman, "Stabilizing a multi machine power system via decentralized feedback linearizing excitation control," IEEE Trans. Power Syst., vol. 8, no. 3, pp.830–839, Aug. 1993.
- [2]. Q. Lu and Y. Sun, "Nonlinear stabilizing control of multi machine systems," IEEE Trans. Power Syst., vol. 4, no. 1, pp. 236–241, Feb. 1989.
- [3]. L. Gao, L. Chen, Y. Fan, and H. Ma, "A nonlinear control design for power systems," Automatica, vol. 28, pp. 975–979, 1992.
- [4]. Y. Wang, D. J. Hill, R. H. Middleton, and L. Gao, "Transient stability enhancement and voltage regulation of power systems," IEEE Trans. Power Syst., vol. 8, no. 2, pp. 620–627, May 1993.
- [5]. Y. Cao and O. P. Malik, "A nonlinear variable structure stabilizer for power system stability," IEEE Trans. Energy Convers., vol. 9, no. 3, pp.489–495, Sep.1994
- [6]. F. K. Mak, "Design of nonlinear generator exciters using differential geometric control theories," in Proc. 31st IEEE Conf. Decision Control, Tucson, AZ, 1992, pp. 1149–1153.
- [7]. C. Zhu, R. Zhou, and Y. Wang, "A new nonlinear voltage regulator for power systems", Int. J. Elect. Power Energy Syst., vol. 19, pp. 19–27, 1997.
- [8]. G. J. Li, T. Lie, C. B. Soh, and G. H. Yang, "Decentralized nonlinear control for stability enhancement in power systems," Proc. Inst. Elect. Eng., Gen., Transm, Distrib., vol. 146, no. 1, pp. 19–24, Jan.1999.
- [9]. B. K. Kumar, S. Singh, and S. Srivastava, "A decentralized nonlinear feedback controller with prescribed degree of stability for damping power system oscillations," Elect. Power Syst. Res., vol. 77, no. 3–4, pp. 204–211, Mar. 2007.
- [10]. Z. Jiang, "Design of a nonlinear power system stabilizer using synergetic control theory," Elect. Power Syst. Res., vol. 79, pp. 855–862, 2009.
- [11]. B. Wang and Z. Mao, "Nonlinear variable structure excitation and steam valving controllers for power system stability," J. Control Theory Appl., vol. 7, no. 1, pp. 97–102, 2009.
- [12]. R. Marino, "An example of a nonlinear regulator," IEEE Trans. Autom. Control, vol. AC-29, no. 3, pp. 276–279, Mar. 1984.
- [13]. M. Ilic and F. K. Mak, "A new class of fast nonlinear voltage controllers and their impact on improved transmission capacity," in Proc. 1989 American Control Conf., 1989, vol. 2, pp. 1246–1251.
- [14]. J. W. Chapman, M. D. Ilic, C. A. King, L. Eng, and H. Kaufman, "Stabilizing a multi machine power system via decentralized feedback linearizing excitation control," IEEE Trans. Power Syst., vol. 8, no. 3, pp.830–839, Aug. 1993.
- [15]. C. A. King, J. W. Chapman, and M. D. Ilic, "Feedback linearizing excitation control on a full-scale power system model," IEEE Trans. Power Syst., vol. 9, no. 2, pp. 1102–1109, May 1994.
- [16]. Y. Guo, D. J. Hill, and Y. Wang, "Global transient stability and voltage regulation for power systems," IEEE Trans. Power Syst., vol. 16, no. 4, pp. 678–688, Nov. 2001
- [17]. D. J. Hill, Y. Guo, M. Larsson, and Y. Wang, "Global Control of Complex Power Systems". Berlin/Heidelberg, Germany: Springer, 2004, vol. 293, Lecture Notes in Control and Information Sciences.
- [18]. F. P. Demello and C. Concordia, "Concepts of synchronous machine stability as affected by excitation control," IEEE Trans. Power App. Syst., vol. PAS-88, no. 4, pp. 316–329, Apr. 1969.
- [19]. J. J. E. Slotine and W. Li, "Applied Nonlinear Control". Englewood Cliffs, NJ: Prentice-Hall, 1991.
- [20]. IEEE Task Force, "Current usage and suggested practices in power system stability simulations for synchronous machines," IEEE Trans. Energy Convers., vol. EC-1, no. 1, pp. 77–93, Mar. 1986.
- [21]. K.R. Padiyar, Power system stability Dynamics and control. New York: Wiley/Interscience, 1996.
- [22]. P. S. Kundur, Power System Stability and Control. New York: McGraw-Hill, 1994.